Am J Physiol Lung Cell Mol Physiol 291: L19–L29, 2006.
First published January 27, 2006; doi:10.1152/ajplung.00306.2005.

Differential induction of apoptosis by cigarette smoke extract in primary human lung fibroblast strains: implications for emphysema

Carolyn J. Baglole,[1,2] Seth M. Bushinsky,[5] Tatiana M. Garcia,[3] Aruna Kode,[1,2] Irfan Rahman,[1,2] Patricia J. Sime,[1,2,4] and Richard P. Phipps[1,2]

[1]*Department of Environmental Medicine,* [2]*Lung Biology and Disease Program,* [3]*Department of Microbiology and Immunology, and* [4]*Division of Pulmonary and Critical Care Medicine, University of Rochester School of Medicine and Dentistry, Rochester, New York; and* [5]*Department of Biological Sciences, Stanford University, Stanford, California*

Submitted 13 July 2005; accepted in final form 21 January 2006

Baglole, Carolyn J., Seth M. Bushinsky, Tatiana M. Garcia, Aruna Kode, Irfan Rahman, Patricia J. Sime, and Richard P. Phipps. Differential induction of apoptosis by cigarette smoke extract in primary human lung fibroblast strains: implications for emphysema. *Am J Physiol Lung Cell Mol Physiol* 291: L19–L29, 2006. First published January 27, 2006; doi:10.1152/ajplung.00306.2005.—Cigarette smoke is the principal cause of emphysema. Recent attention has focused on the loss of alveolar fibroblasts in the development of emphysema. Fibroblasts may become damaged by oxidative stress and undergo apoptosis as a result of cigarette smoke exposure. Not all smokers develop lung diseases associated with tobacco smoke, a fact that may reflect individual variation among human fibroblast strains. We hypothesize that fibroblasts from different human beings vary in their ability to undergo apoptosis after cigarette smoke exposure. This could account for emphysematous changes that occur in the lungs of some but not all smokers. Primary human lung fibroblast strains were exposed to cigarette smoke extract (CSE) and assessed for viability, morphological changes, and mitochondrial transmembrane potential as indicators of apoptosis. We also examined the generation of intracellular reactive oxygen species (ROS), 4-hydroxy-2-nonenal, and changes in glutathione (GSH) and glutathione disulfide (GSSG) levels. Each human lung fibroblast strain exhibited a differential sensitivity to CSE as judged by changes in mitochondrial membrane potential, viability, ROS generation, and glutathione production. Interestingly, the thiol antioxidants *N*-acetyl-L-cysteine and GSH eliminated CSE-induced changes in fibroblast morphology such as membrane blebbing, nuclear condensation, and cell size and prevented alterations in mitochondrial membrane potential and the generation of ROS. These findings support the concept that oxidative stress and apoptosis are responsible for fibroblast death associated with exposure to tobacco smoke. Variations in the sensitivity of fibroblasts to cigarette smoke may account for the fact that only some smokers develop emphysema.

mitochondrial membrane potential; reactive oxygen species; glutathione; 4-hydroxy-2-nonenal

CHRONIC OBSTRUCTIVE PULMONARY disease (COPD) is the fourth leading cause of death in the United States (43). Emphysema, an important component of COPD, is an irreversible lung disorder characterized by inflammation and the permanent, destructive enlargement of respiratory bronchioles and surrounding alveoli (55). Although there are numerous risk factors associated with developing COPD, the most prominent factor is cigarette smoking, which is linked to 95% of all cases of emphysema (43).

Cigarette smoke is a complex mixture containing over 4,800 compounds and is a potent oxidant (8), yielding an estimated 1×10^{17} oxidant molecules per puff. Oxidative stress caused by cigarette smoking can result in destruction of the alveolar wall (21, 32), leading to airway enlargement, a central feature in the development of emphysema, by triggering the apoptotic pathway (58). Apoptosis is a form of death whereby cells are removed from a tissue in a controlled manner. Apoptosis plays an important role in embryonic development and tissue homeostasis, as well as in pathological conditions such as cancer (44). Cells that are undergoing apoptosis exhibit characteristics such as membrane blebbing, cell shrinkage, formation of apoptotic bodies (4), and changes in mitochondrial membrane potential ($\Delta\Psi_m$) (2, 29, 42).

Cigarette smoke causes apoptosis in the human monocytic cell line U-937 (61), human umbilical vein endothelial cells (64), alveolar macrophages (1), and the HFL-1 fibroblast strain (4, 22). Fibroblasts are key structural cells within the lung whose primary function is the production of extracellular matrix for tissue maintenance and repair. Fibroblasts are a target for cigarette smoke-induced damage; loss of fibroblasts due to smoke-induced apoptosis represents a potential mechanism for the development of COPD and emphysema. Furthermore, fibroblasts are thought to be targets of the water-soluble components of cigarette smoke that pass through the basement membrane (22). Curiously, only 15–20% of smokers develop COPD (53), a factor that may reflect individual genetic differences. We hypothesize that human lung fibroblast strains isolated from different human beings vary in their sensitivity to cigarette smoke. With the use of markers of viability, oxidative stress, and apoptosis, the results presented here reveal that human lung fibroblast strains differ greatly in their sensitivity to cigarette smoke.

MATERIALS AND METHODS

Chemicals. N-acetyl-L-cysteine (NAC), glutathione reduced ethyl ester, 3-(4,5-dimethylthiazol-2-yl)-2,5-diphenyltetrazolium bromide (MTT), 5,5′-dithiobis[2-nitrobenzoic acid] (DTNB), β-nicotinamide adenine dinucleotide phosphate (β-NADPH), glutathione reductase, sulfosalicylic acid, Mayer's hematoxylin solution, and Eosin Y were obtained from Sigma (St. Louis, MO). 5-(-6)-Carboxy-2′,7′-dichlorodihydrofluorescein diacetate (H_2DCFDA) and 3,3′-dihexyloxacarbocyanine iodide ($DiOC_6$) were obtained from Molecular Probes (Eugene, OR).

Address for reprint requests and other correspondence: R. P. Phipps, Univ. of Rochester School of Medicine and Dentistry, Dept. of Environmental Medicine, 601 Elmwood Ave, Box 850, Rochester, NY 14642 (e-mail: richard_phipps@urmc.rochester.edu).

The costs of publication of this article were defrayed in part by the payment of page charges. The article must therefore be hereby marked "*advertisement*" in accordance with 18 U.S.C. Section 1734 solely to indicate this fact.

Cell culture. Human fetal lung fibroblasts (HFL-1) were purchased from American Type Culture Collection (Manassas, VA). The primary human lung fibroblast strains CH1, LZZ, CH2, and L828 were established as previously described (12) from lung biopsies of morphologically normal lung by a tissue explant technique. These cells were identified as fibroblasts by their morphology, adherent nature, expression of vimentin and type I and III collagen, and lack of expression of cytokeratin, α-smooth muscle actin, factor VIII, and CD45. All experiments were conducted with minimum essential medium (MEM) supplemented with 2 mM glutamine (Invitrogen, Carlsbad, CA) and 10% FBS (Hyclone Labs, Logan, UT) unless otherwise indicated. Cells were maintained at 37°C and incubated in humidified 5% CO_2-95% air. Fibroblasts were used before *passage 14*.

Preparation of cigarette smoke extract. Research-grade cigarettes (1R3F) with a filter were obtained from the Kentucky Tobacco Research Council (Lexington, KY) and smoked to 0.5 cm above the filter with a modification of the method developed by Carp and Janoff (5). Briefly, cigarette smoke extract (CSE) was prepared by bubbling smoke from 2 cigarettes into 20 ml of serum-free MEM at a rate of 1 cigarette/min as previously described (37, 38). The pH of the MEM was adjusted to 7.4, and the medium was sterile filtered with a 0.45-μm filter (25-mm Acrodisc; Pall, Ann Arbor, MI). The CSE (called 100%) was prepared no more than 24 h in advance and stored at 4°C. To ensure consistency in the CSE between experiments, measurements of optical density were taken at a wavelength of 320 nm immediately after preparation of the CSE. The CSE was diluted to the appropriate concentration in serum-free MEM; all experiments were conducted with this medium.

Histochemistry. To assess morphological changes following smoke exposure, cells were seeded onto eight-well chamber slides (BD Biosciences, San Diego, CA) at a density of 5,000 cells/well and left undisturbed for 24 h. Cells were then switched to serum-free medium for 24 h and treated with 10% CSE or medium alone (control) for 6 h. In parallel experiments, some wells were pretreated with 1 mM NAC for 1 h, followed by coincubation with 10% CSE for 6 h. Hematoxylin and eosin staining was performed according to standard histological protocols. Briefly, the cells were washed once with PBS and fixed in 4% paraformaldehyde with 0.5% Tween 20 for 10 min. Slides were then rinsed with water and stained with hematoxylin. After several rinses with water, slides were dipped in ammonia water, rinsed, and stained with eosin. Finally, cells were rinsed in water and coverslipped in Immu-mount (Shandon, Pittsburgh, PA). Cells were viewed with an Olympus BX51 microscope (New Hyde Park, NY) and photographed with a SPOT camera with SPOT RT software (New Hyde Park, NY).

Viability. MTT assay was performed to assess cell viability after cigarette smoke exposure. MTT is reduced to a colored product in metabolically active, living cells with a functional mitochondria (20), producing the typical purple product, and is therefore indicative of cell viability. Equivalent numbers of fibroblasts were cultured in triplicate in flat-bottomed 96-well plates (Falcon, Becton-Dickinson, Lincoln Park, NJ) until they reached 70% confluence. Fibroblasts were serum starved for 24 h before treatment with 140 μl/well of varying concentrations of CSE for 3, 6, 24, and 48 h. After this, 10 μl of a 5 mg MTT in PBS solution was added to each well. After incubating for 4 h at 37°C, the plate was centrifuged, the medium was removed, and the insoluble precipitate was dissolved by adding 200 μl of DMSO to each well. The plates were read with a BioRad microplate reader at 510 nm.

Measurement of reactive oxygen species and apoptosis by flow cytometry. Oxidative stress was measured in lung fibroblasts with CSE by using H_2DCFDA, a cell-permeant indicator for reactive oxygen species (ROS) that is nonfluorescent until oxidation occurs within the cell (11, 54). Flow cytometric analysis of apoptosis included assessment of mitochondrial activity with $DiOC_6$, a dye that strongly labels active mitochondria in living cells. Changes in cell size and granularity were determined by forward and side scatter profiles. For these experiments, equivalent numbers of cells were grown to confluence in 25-cm^2 cell culture flasks, serum starved for 24 h, and then treated with 5% and 10% CSE for either 3 (ROS) or 6 (apoptosis) h. Some flasks were treated with 1 mM NAC for 1 h before and during treatment with CSE or with 5 mM GSH reduced ethyl ester for 2 h before treatment with CSE. Controls included incubation with NAC only or incubation with serum-free medium alone with and without H_2DCFDA or $DiOC_6$. For $DiOC_6$, after treatment $DiOC_6$ was added at a final concentration of 40 nM for 15 min at 37°C. Cells were then harvested by trypsinization, washed, and resuspended in 0.5 ml of PBS. For H_2DCFDA, after treatment cells were washed with PBS and H_2DCFDA (10 μM) was added for 20 min at 37°C. Cells were then trypsinized, washed, and resuspended in PBS. Flow cytometric analysis was performed with a Becton-Dickinson FACSCalibur flow cytometer (BD Biosciences, Mountain View, CA). A minimum of 10,000 events were acquired for each sample. Debris was gated out, and analysis was performed only on the fibroblast population.

Immunocytochemistry. Fibroblasts were seeded on eight-well glass chamber slides at a density of 5×10^3 cells/well and allowed to adhere for ~72 h. After this, cells were treated with 5% or 10% CSE for 3 h. Cells maintained in serum-free MEM were used as negative control. After being treated, cells were washed once with PBS, fixed with 3% H_2O_2 for 15 min, and blocked with 5% normal horse serum. The antibody against 4-hydroxy-2-nonenal (4-HNE) (OxisResearch, Portland, OR) was diluted in PBS-BSA to 10 μg/ml and incubated overnight at 4°C. To assess the level of nonspecific staining, cells were incubated under the same conditions with the mouse IgG1 isotype antibody. Biotinylated anti-mouse IgG antibody was used for secondary binding (1:200) and incubated for 1 h at room temperature before being incubated with streptavidin-horseradish peroxidase. Antibody binding was visualized with the substrate aminoethylcarbazole (Zymed, South San Francisco, CA).

Measurement of intracellular GSH and GSSG levels. Human lung fibroblast strains grown to confluence in 25-cm^2 cell culture flasks were treated either with control medium or with 5% CSE for 3, 6, and 24 h. To determine whether GSH was increased after treatment with the GSH ethyl ester, confluent flasks of fibroblast strains HFL-1, L828, and CH2 were treated with 5 mM GSH reduced ethyl ester for 2 h. After treatments, monolayers of fibroblasts were washed with 2 ml of ice-cold PBS and scraped into 300 μl of ice-cold extraction buffer (0.1% Triton X-100, 0.6% sulfosalicylic acid in 0.1 M phosphate buffer with 5 mM EDTA, pH 7.5). Cells were vortexed for 20 s, followed by sonication (30 s) and centrifugation (2,000 rpm for 5 min at 4°C). Determination of total intracellular levels of GSH was performed as originally described by Tietze (57) with DTNB-GSSG/glutathione reductase recycling (23). For the GSSG assay, the supernatant was treated with 2-vinylpyridine and triethanolamine as previously described (13, 51). Results are expressed in nanomoles of GSSG per microgram of protein.

Statistical analysis. Statistical analysis was performed with Statview V5.0 (SAS Institute, Cary, NC), and ANOVA with Fisher's post hoc test was used to assess differences between multiple treatment groups.

RESULTS

CSE differentially reduces viability in normal human lung fibroblast strains. To determine the effect of CSE on viability of lung fibroblasts established from different human beings, normal human lung fibroblast strains were treated with increasing concentrations of CSE for 3, 6, 24, and 48 h and cell viability was assessed with the colorimetric MTT assay. Viability was not significantly reduced by incubation with CSE (to 20%) for 3 or 6 h. Changes in viability were observed with incubation with increasing concentrations of CSE for 24 h, and reductions in viability were maximum at 48 h. At this time

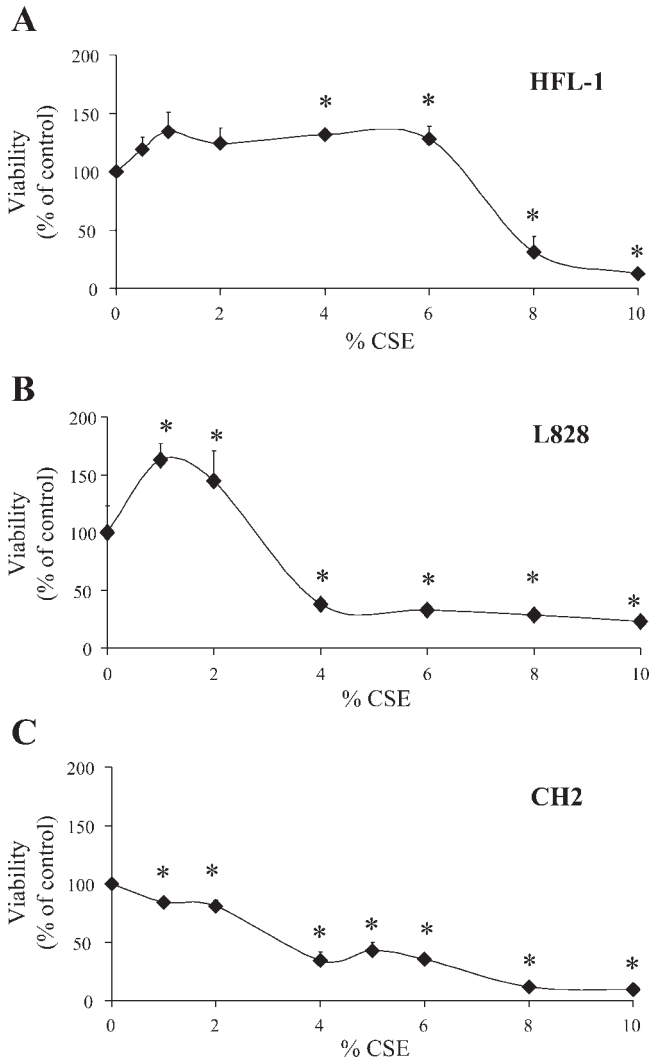

Fig. 1. Cigarette smoke extract (CSE) significantly reduces viability in human lung fibroblasts. Fibroblast strains generated from different individuals were exposed to increasing concentrations of CSE, and viability was assessed by 3-(4,5-dimethylthiazol-2-yl)-2,5-diphenyltetrazolium bromide (MTT) assay as described in MATERIALS AND METHODS. There was a significant increase in mitochondrial activity in the fibroblast strains HFL-1 (*A*) and L828 (*B*) at low CSE concentrations. In the 3 human lung fibroblast strains tested, viability was significantly reduced when fibroblasts were incubated with 8% (HFL-1, *A*), 4% (L828, *B*), and 1% (CH2, *C*) CSE. *$P < 0.05$ compared with untreated fibroblasts.

point, lower concentrations of CSE induced an apparent rise in mitochondrial activity in the fibroblast strains HFL-1 and L828 (Fig. 1, *A* and *B*), but not CH2 (Fig. 1*C*), that was not indicative of an increase in cell number. CSE reduced cell viability in a dose-dependent manner in all human lung fibroblast strains tested (Fig. 1). There was no further reduction in viability in the L828 and CH2 fibroblast strains beyond exposure to 4% (Fig. 1*B*) and 8% (Fig. 1*C*) CSE, respectively. Viability was significantly reduced (compared with untreated cells) when fibroblasts were exposed to 8% (HFL-1, Fig. 1*A*), 4% (L828, Fig. 1*B*), and 1% (CH2, Fig. 1*C*) CSE.

The reduction in viability was also significantly different among fibroblast strains when two additional strains (LZZ and CH1) were evaluated and exposed to 5% CSE (Fig. 2). The decrease in viability was significantly different among the normal human lung fibroblast strains CH2, CH1, and LZZ compared with HFL-1. Furthermore, in the most sensitive fibroblast strain, CH2, there was a significant difference in viability compared with the CH1 and LZZ strains. Collectively, these data strongly suggest that fibroblasts established from different human beings vary in their sensitivity to cigarette smoke. Because viability of human lung fibroblasts was significantly reduced by exposure of some strains to 5% CSE whereas others showed a reduction in viability to concentrations approaching 10% CSE, further experiments were conducted with CSE at both 5% and 10%.

CSE induces morphological changes characteristic of apoptosis in normal human lung fibroblasts. Apoptosis is characterized by morphological parameters such as cellular shrinkage and membrane blebbing (34, 62). To assess whether CSE induced membrane blebbing in human lung fibroblasts, fibroblast strains were exposed to CSE and changes in cell architecture were assessed by light microscopy. After 6 h of incubation, 10% CSE induced apoptotic morphological changes in human lung fibroblasts (Fig. 3). In both HFL-1 (Fig. 3, *A* and *C*) and L828 (Fig. 3, *B* and *D*) fibroblast strains treated with 10% CSE, membrane blebbing and nuclear condensation were evident, suggesting apoptotic cell death.

Cells that are undergoing apoptosis have a reduction in cell volume (41), an early prerequisite hallmark that eventually leads to cell death (36, 44). Therefore, to further assess apoptosis following CSE exposure, fibroblasts were exposed to 10% CSE for 6 h and their size and granularity were assessed by flow cytometry. A minimum of 10,000 cells were acquired and analyzed per sample. Fibroblasts that were untreated were uniform in size and granularity and were evident as a single population of cells based on their dot plot profiles of forward and side scatter (Fig. 4, *left*, *R3*). It was also evident in all dot plot profiles of untreated fibroblasts that there were two additional regions, *R1* and *R2* (Fig. 4, *left*). These two regions likely consisted of cellular debris (*R1*) and fibroblasts of slightly smaller size (*R2*). In all fibroblast strains tested, exposure of the cells to 10% CSE caused a dramatic decrease in cell size, as evidenced by a decrease in the forward scatter (Fig. 4, *right*),

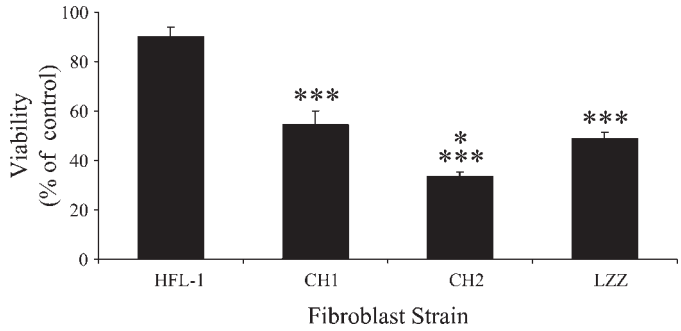

Fig. 2. Human lung fibroblast strains exhibit differential viability in response to CSE. Four normal human lung fibroblast strains from different individuals were exposed to 5% CSE, and viability was assessed by MTT assay. The reduction in viability caused by exposure to 5% CSE was significantly different among the fibroblast strains. The reduced viability exhibited by fibroblast strains CH1 (54.4 ± 5.6%), CH2 (33.3 ± 2.1%), and LZZ (48.7 ± 2.8%) was significantly different compared with the HFL-1 fibroblast strain (89.8 ± 4.2%) (***$P < 0.0001$). The reduction in viability exhibited by the most sensitive fibroblast strain, CH2, was also significantly different compared with the fibroblast strains LZZ and CH1 (*$P < 0.05$). Values are expressed as mean ± SE % of control.

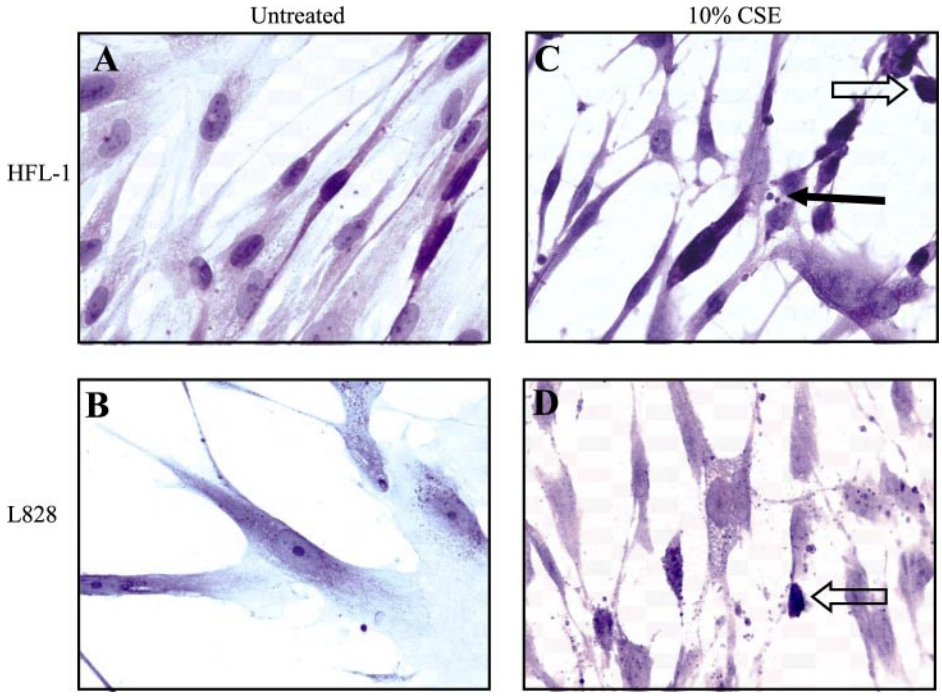

Fig. 3. CSE-induced morphological changes, characteristic of apoptosis, in 2 strains of human lung fibroblasts, HFL-1 and L828. Human lung fibroblast strains HFL-1 and L828 were treated with 10% CSE for 6 h, and morphology was assessed by hematoxylin and eosin staining as described in MATERIALS AND METHODS. Untreated fibroblasts exhibit typical fibroblastic morphology (*A* and *B*), whereas those treated with 10% CSE display morphological features of apoptosis including membrane blebbing (solid arrow) and nuclear condensation (open arrows in *C* and *D*) (magnification ×60). Data are representative of 3 separate experiments.

indicative of cigarette smoke-induced apoptosis. This reduction in cell size dramatically decreased the percentage of cells within *region R3*. Here, the decline in the percentage of fibroblasts varied, ranging from −32.3% to −51.5% (Fig. 4, *right*, *R3*). This decrease in cell size also caused a corresponding increase in the percentage of fibroblasts with *regions R1* and *R2*. This increase in the percentage of cells within the intermediate *region R2* ranged from +6.7% to +9.6% (Fig. 4, *right*, *R2*). The percentage of apoptotic fibroblasts in *region R1* also exhibited a corresponding increase on exposure to 10% CSE, indicating CSE-induced apoptosis. Here, this increase ranged from +24.1% to +41.1% (Fig. 4, *right*, *R1*). The fibroblast strain CH2 had the highest percentage (41.1%) of apoptotic cells after exposure to 10% CSE, indicating that fibroblast strains vary in their sensitivity to CSE.

CSE reduces mitochondrial $\Delta\Psi_m$ and generates ROS. Mitochondrial membrane permeabilization is an essential step leading to apoptosis. Disruption of $\Delta\Psi_m$ irreversibly commits cells to undergo death (29) and is an early marker of apoptosis (42). Furthermore, cigarette smoke was previously shown to induce mitochondrial depolarization in human monocytes (2). Therefore, reduced $\Delta\Psi_m$, as measured by diminished incorporation of the fluorescent dye $DiOC_6$, was used as an early indicator for CSE-induced apoptosis. Fibroblasts were cultured in the presence of CSE or control medium for 6 h, and $DiOC_6$ incorporation was measured by flow cytometry. Although CH2 had a slightly lower baseline fluorescence when untreated cells were incubated with the dye alone, there was no significant difference in baseline fluorescence (mean fluorescence intensity) among the three fibroblast strains (HFL-1: 884.8 ± 170; L828: 747.6 ± 429; CH2 390.7 ± 163). When fibroblasts were exposed to 5% CSE, there was a slight reduction in $\Delta\Psi_m$ in all strains tested (Fig. 5*A*). For two strains of fibroblasts, HFL-1 and L828, this percentage of CSE reduced $\Delta\Psi_m$ to 78.5 ± 9.0% and 68.6 ± 26.5%, respectively, compared with untreated cells. Of the three fibroblast strains tested, CH2 fibroblasts exhibited the least decrease, 87.9 ± 11.8% (Fig. 5*A*). However, when exposed to 10% CSE, HFL-1 and L828 fibroblasts exhibited a significant reduction in $\Delta\Psi_m$ (Fig. 5*B*, $P < 0.05$), as indicated by reduced incorporation of $DiOC_6$, supporting CSE-induced apoptosis in human lung fibroblasts. In addition, this decrease in $\Delta\Psi_m$ exhibited by L828 fibroblasts was significantly different compared with the fibroblast strain HFL-1 ($P < 0.05$), indicating that fibroblast strains vary in their apoptotic response to cigarette smoke.

At moderate concentrations, ROS are classic signals for death by apoptosis (2). We therefore tested the ability of 5% and 10% CSE to induce the generation of ROS in human lung fibroblasts, using flow cytometry to measure the oxidation of the chemical probe H_2DCFDA (see Fig. 6). Fluorescein derivatives such as H_2DCFDA can be oxidized by a variety of oxidants, including reactive nitrogen species, and are widely referenced indicators of oxidative stress and ROS production (4, 6, 14). Basal ROS production (mean fluorescence intensity) was not significantly different among the fibroblast strains (HFL-1: 7.1 ± 0.9; L828: 8.9 ± 2.3; CH2: 7.6 ± 1.5). At 5% CSE, however, there was a significant increase in the production of ROS in the human lung fibroblast strains CH2 and L828 (134 ± 5.6% and 130.2 ± 14.3%, respectively; $P < 0.05$) but not HFL-1 (Fig. 6*A*). However, when fibroblasts were cultured in the presence of 10% CSE, a significant increase in the generation of ROS occurred in all fibroblast strains tested, with the greatest increase occurring in the CH2 strain (Fig. 6*B*; $P < 0.05$). In the CH2 strain, 10% CSE induced nearly an 80% increase in ROS levels. This increase in ROS was significantly different compared with all other fibroblast strains (Fig. 6*B*; $P < 0.05$).

CSE induces lipid peroxidation in human lung fibroblast strains. Membrane lipid peroxidation is a consequence of oxidative stress (52). 4-HNE, a specific product of lipid per-

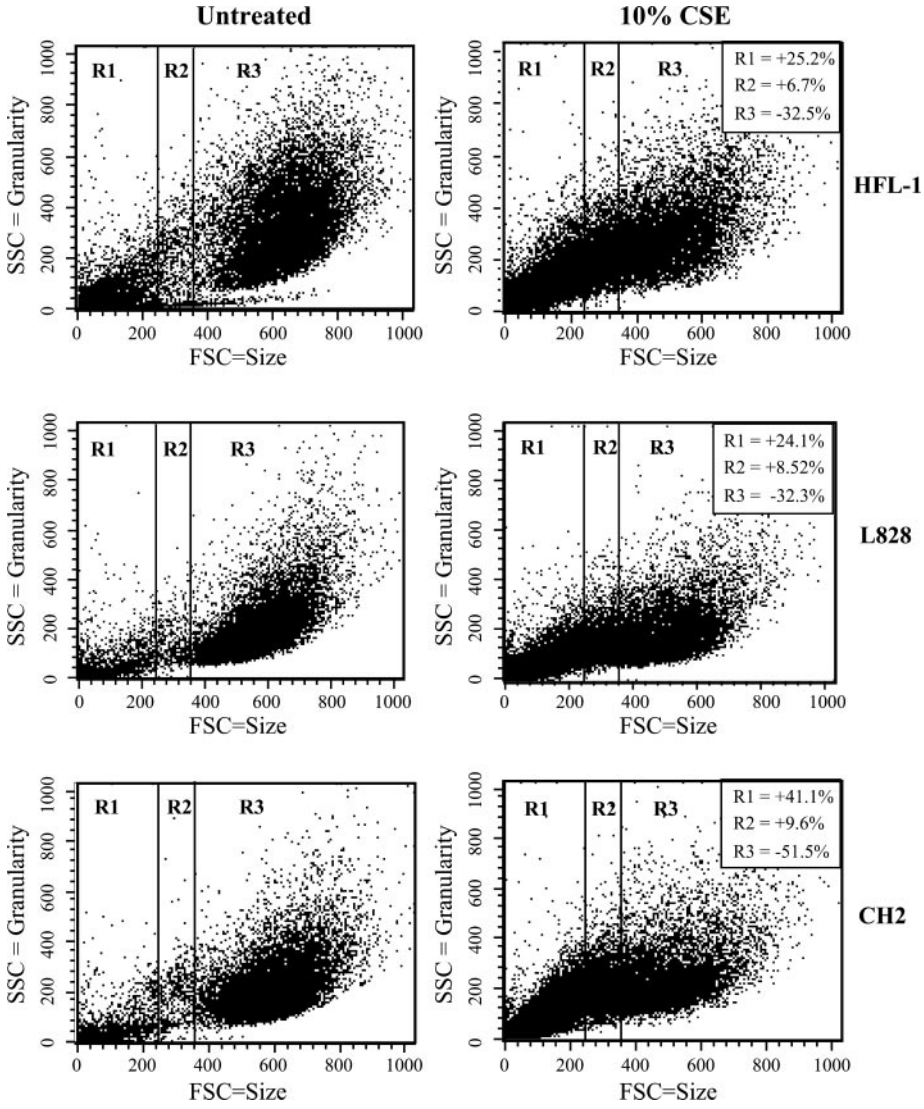

Fig. 4. CSE alters human lung fibroblast cell size. Three strains of human lung fibroblasts were untreated (*left*) or cultured in the presence of 10% CSE (*right*) for 6 h, and change in cell size was assessed by flow cytometry as described in MATERIALS AND METHODS. Ten thousand cells per sample were acquired. Changes in the percentage of cells within *regions R1*, *R2*, and *R3* of the dot plots on exposure to 10% CSE, indicative of CSE-induced apoptosis, were determined. Treatment with 10% CSE induced a decrease in the percentage of cells within *region R3* in fibroblast strains HFL-1, L828, and CH2 as determined by a decrease in the forward scatter (FSC). A corresponding increase in the percentage of apoptotic fibroblasts occurred in both intermediate *region R2* as well as *region R1*. Note the variability in the sensitivity of the fibroblast strains. SSC, side scatter.

oxidation, is generated in response to oxidative stress and is elevated in the lungs of patients with COPD (52). Thus we examined the ability of CSE to induce lipid peroxidation by assessing the intensity of 4-HNE staining in human lung fibroblasts that were exposed to control medium or to 5% or 10% CSE for 3 h. No cellular staining was observed in the isotype controls (data not shown). In both lung fibroblast strains tested, HFL-1 and CH2, diffuse staining (red color) was evident in the cytoplasm of cells that were exposed to control medium. Staining in the nucleus and nuclear membrane of these control-treated fibroblasts was minimal (Fig. 7, *top*). However, with exposure to both 5% and 10% CSE, there was an increase in the intensity of cytoplasmic staining (Fig. 7, *middle* and *bottom*, closed arrows) in both fibroblast strains, indicative of an increase in 4-HNE. These was also an increase in 4-HNE in both the nucleus and the nuclear membrane, as evidenced by the heightened staining (Fig. 7, *middle* and *bottom*, open arrows). These data suggest that CSE increases 4-HNE production as a consequence of oxidative stress.

CSE reduces GSH levels in human lung fibroblast strains. GSH, an important antioxidant in the lung (49), has been implicated in various cellular process, including apoptosis (27). We therefore examined GSH levels in human lung fibroblast strains exposed to 5% CSE for 3, 6, and 24 h. Baseline GSH values (nmol GSH/μg protein) were similar among the three fibroblast strains (HFL-1: 9.7 ± 0.43; CH2: 8.9 ± 0.13; L828: 10.2 ± 0.27). All fibroblast strains exhibited an initial decrease in intracellular GSH levels when exposed to 5% CSE for 3 h (Fig. 8), with the CH2 fibroblast strain exhibiting the largest decline in GSH levels (29.9 ± 14.25%) compared with control levels. By 24 h, GSH returned to near-baseline levels in the more CSE-resistant HFL-1 fibroblast strain (90.9 ± 2.3%). However, GSH levels in the other two CSE-treated fibroblast strains failed to return to baseline, only recovering to between 69.8% and 66.7% (L828 and CH2, respectively) of untreated cells.

To ascertain whether the decrease in GSH levels occurred with a concomitant increase in GSSG, we assayed for GSSG levels in two human lung fibroblast strains that were cultured in the presence or absence of 5% CSE. Cells that were untreated had baseline GSSG levels (nmol/μg protein) of 0.78 ± 0.28 for the CH2 fibroblast strain and 0.58 ± 0.01 for the HFL-1 fibroblast strain. Treatment with 5% CSE for 3, 6, or 24 h did not signifi-

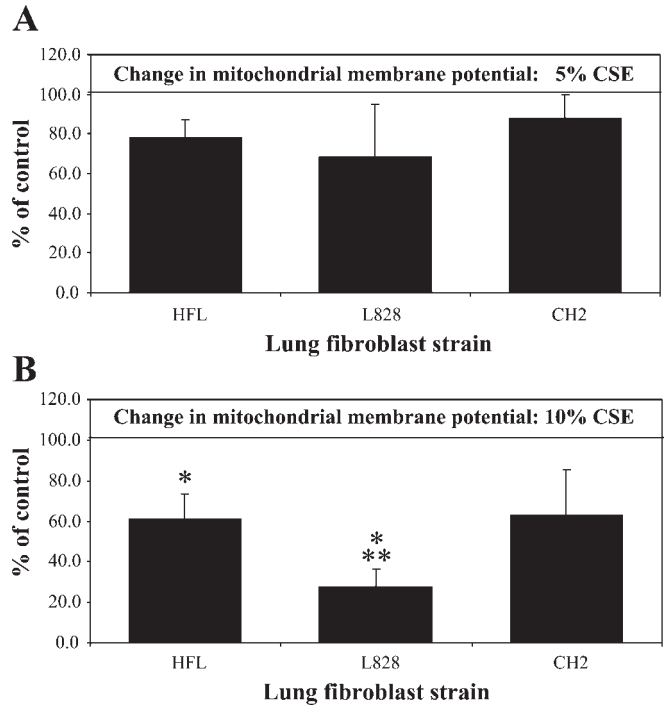

Fig. 5. CSE differentially reduces mitochondrial transmembrane potential ($\Delta\Psi_m$) in human lung fibroblasts. Three strains of human lung fibroblasts were untreated or were cultured in the presence of 5% or 10% CSE for 6 h, and changes in the mitochondrial $\Delta\Psi_m$ were assessed by flow cytometry as described in MATERIALS AND METHODS. *A*: a slight reduction in 3,3′-dihexyloxacarbocyanine iodide ($DiOC_6$) incorporation, as indicated by decreased fluorescence intensity, was evident in human lung fibroblast strains HFL-1 (78.5 ± 9.0%), L828 (68.6 ± 26.4%), and CH2 (87.9 ± 11.8%) when these cells were exposed to 5% CSE. *B*: exposure of fibroblast strains HFL-1 and L828 to 10% CSE resulted in a significant decrease in $\Delta\Psi_m$ (*$P < 0.005$ compared with control). The decrease in $\Delta\Psi_m$ exhibited by the strain L828 was significantly lower compared with HFL-1 (**$P < 0.05$). Results are presented as means ± SE fluorescent intensity (n = 2–8).

cantly change GSSG levels in CH2 (0.60 ± 0.1, 0.63 ± 0.07, and 0.86 ± 0.02 nmol/μg protein, respectively) or HFL-1 (0.43 ± 0.02, 0.31 ± 0.23, and 0.6 ± 0.04 nmol/μg protein, respectively) fibroblasts. These data indicate that CSE does not alter the levels of GSSG in human lung fibroblast strains.

Prevention of CSE-induced apoptosis by antioxidants NAC and GSH. NAC, also an antioxidant, can serve as a precursor to GSH synthesis (27). Because CSE can induce the generation of ROS and induce apoptosis in human fibroblast strains, we examined the role of antioxidants in CSE-induced apoptosis. To determine whether the effects of CSE could be ablated by treatment with the antioxidant NAC, we pretreated fibroblasts with NAC in the presence or absence of CSE and assessed morphological parameters, $\Delta\Psi_m$, and the production of ROS as described above. Histological assessment of human lung fibroblast strains HFL-1 and L828 revealed that pretreatment with 1 mM NAC ablated the morphological indicators of apoptosis including cell shrinkage and membrane blebbing (data not shown) that were evident when cells were incubated with 10% CSE alone (see also Fig. 3, *C* and *D*). Here, treatment with NAC resulted in fibroblast morphology that was not different from controls (data not shown).

NAC was also able to prevent the CSE-induced loss of $\Delta\Psi_m$ and generation of ROS. Incubation of cells with NAC alone did not affect $\Delta\Psi_m$ compared with cells incubated with medium. Pretreatment with 1 mM NAC abrogated the CSE-induced loss of fluorescence intensity of $DiOC_6$ at both 5% CSE (data not shown) and 10% CSE in fibroblast strains HFL-1 (Fig. 9*A*), L828 (Fig. 9*B*), and CH2 (data not shown), indicating that NAC prevented the ability of CSE to alter $\Delta\Psi_m$. In addition to the preventative effects on mitochondrial function, NAC also dramatically attenuated the production of ROS in all human lung fibroblast strains tested (Fig. 10, *left*). Here, pretreatment with 1 mM NAC reduced the CSE-induced generation of ROS.

In separate experiments, fibroblast strains were also pretreated with 5 mM GSH followed by treatment with 5% or 10% CSE. GSH is not readily transported into most cells. Instead, we used a GSH reduced ethyl ester, which is more lipophilic and passes readily into cells and is hydrolyzed to GSH by nonspecific esterases (35). Incubation of lung fibroblast strains with the GSH reduced ethyl ester increased intracellular GSH levels by as much as 57% (data not shown). Exogenously administrated GSH completely prevented the generation of ROS by both 5% CSE (data not shown) and 10% CSE (Fig. 10, *right*) in all of the fibroblast strains. Here, the flow cytometry

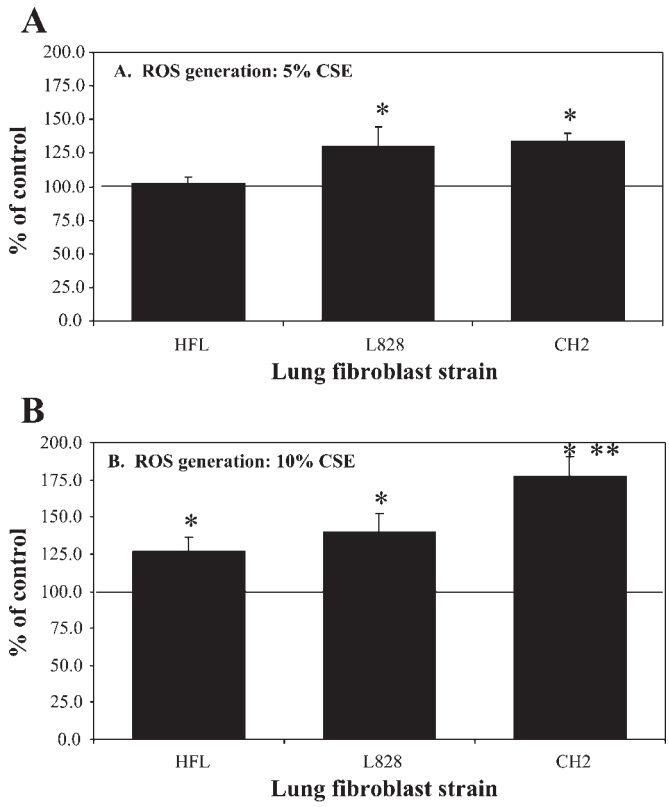

Fig. 6. CSE differentially induces the generation of reactive oxygen species (ROS) in human lung fibroblast strains. Fibroblast strains HFL-1, L828, and CH2 were incubated with 5% or 10% CSE for 3 h and examined for the generation of ROS by the oxidation of 5-(-6)-carboxy-2′,7′-dichlorodihydrofluorescein diacetate (H_2DCFDA) as described in MATERIALS AND METHODS. *A*: on exposure to 5% CSE, there was a significant increase in the generation of ROS in fibroblast strains L828 and CH2 compared with untreated and fibroblast strain HFL-1 (*$P < 0.05$) but not in HFL-1 compared with untreated. *B*: exposure to 10% CSE caused a significant increase in ROS production in all fibroblast strains tested (*$P < 0.05$) compared with untreated controls. The amount of ROS generation by the fibroblast strain CH2 was significantly greater (~77%) compared with L828 and HFL-1 fibroblast strains (**$P < 0.05$). Results are expressed as means ± SE fluorescent intensity (n = 2–5).

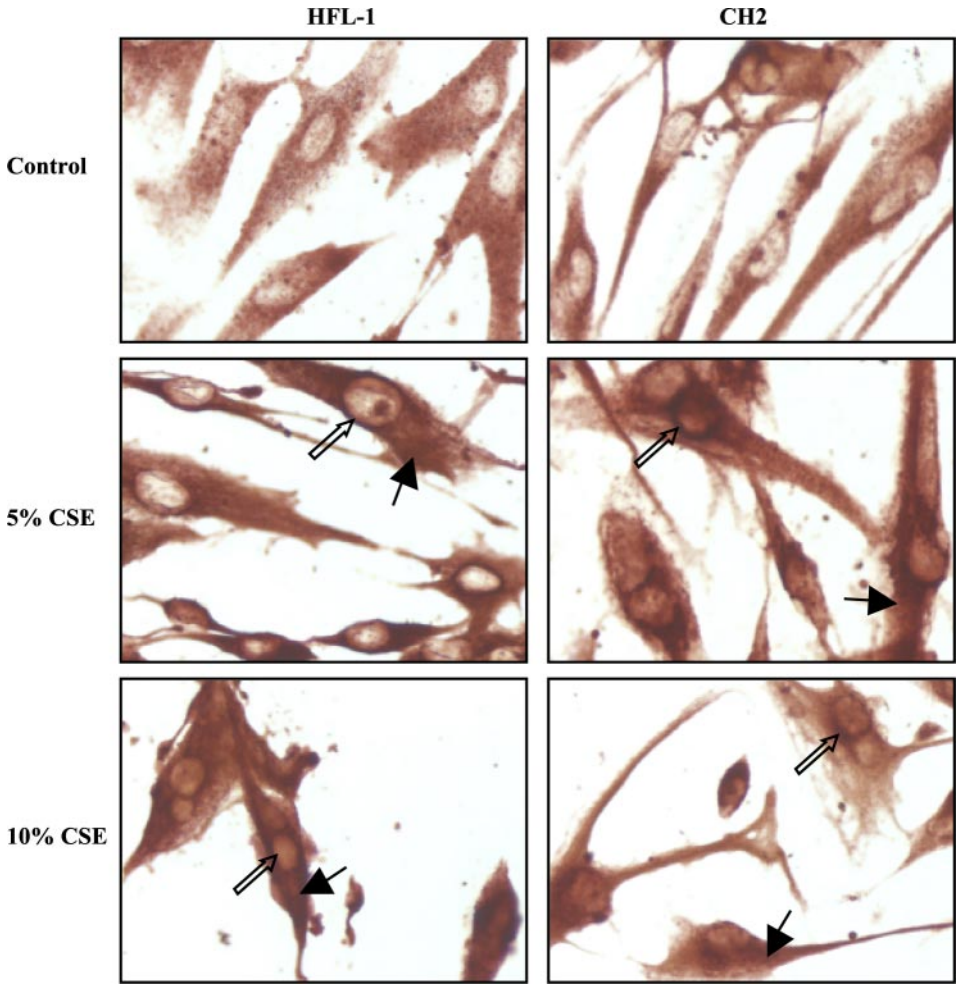

Fig. 7. Production of 4-hydroxy-2-nonenal (4-HNE) is induced by CSE in human lung fibroblasts. Fibroblast strains HFL-1 and CH2 were exposed to 5% and 10% CSE for 3 h, and lipid peroxidation was assessed by immunocytochemical staining with an antibody against 4-HNE as described in MATERIALS AND METHODS. Cells that were treated with control medium had light cytoplasmic and nuclear staining (*top*) that was remarkably increased when the fibroblasts were exposed to 5% or 10% CSE (*middle* and *bottom*, respectively). Staining of the nuclear membrane was also increased in the CSE-treated fibroblasts (*middle* and *bottom*, open arrows).

histograms of untreated and GSH-treated fibroblasts could be superimposed. Collectively, these data indicate that CSE is able to differentially induce apoptosis in human lung fibroblast strains, likely through the generation of ROS.

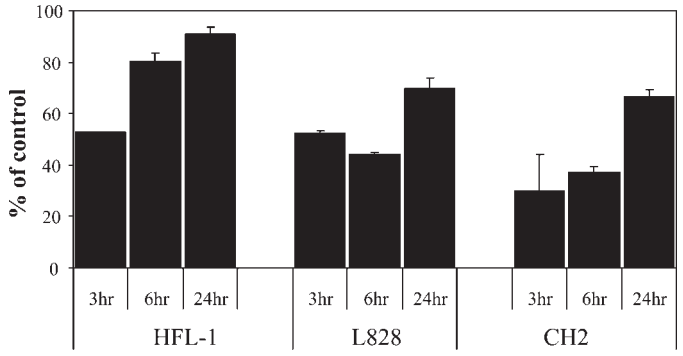

Fig. 8. CSE reduces glutathione (GSH) levels in human lung fibroblast strains. Human lung fibroblast strains were untreated or exposed to 5% CSE for 3, 6, or 24 h, and intracellular GSH levels were measured as described in MATERIALS AND METHODS. Baseline GSH values were similar among the 3 fibroblast strains (8.9 ± 0.13 to 10.2 ± 0.27 nmol GSH/μg protein). GSH initially decreased in all fibroblast strains when exposed to 5% CSE (3 h) (% of control: 29.95 ± 14.25 to 52.63 ± 0.18) but recovered by 24 h in the CSE-resistant HFL-1 fibroblast strain (90.9 ± 2.7). Although GSH levels increased over time in the CH2 and L828 strains, they failed to return to control values in these 2 fibroblast strains (66.7 ± 2.72 and 69.79 ± 3.9, respectively). Values are expressed as means ± SE ($n = 2$).

DISCUSSION

We report here the differential induction of apoptosis in normal human lung fibroblasts established from different human beings, a novel finding that reflects individual genetic diversity in sensitivity to cigarette smoke. Moreover, we used markers of apoptosis such as viability, morphological parameters, changes in cell size, alterations in $\Delta\Psi_m$, and ROS generation to demonstrate that the fibroblast strain HFL-1 appears to be the least sensitive to CSE. HFL-1 is an easy-to-grow and commercially available fibroblast strain that is commonly used to assess the affects of CSE on fibroblasts (4, 22, 26, 40). Our results are consistent with a recent study by Carnevali and colleagues (4), who established that HFL-1 cells do apoptose and exhibit signs of oxidative stress after exposure to CSE. However, in our study, HFL-1 exhibited significantly lower sensitivity to CSE compared with other primary lung fibroblast strains that were established from different individuals. Although all of the fibroblasts strains exhibited signs of apoptosis, HFL-1 were the least sensitive (Fig. 2), requiring a higher percentage of CSE to reduce viability to 50% (Fig. 1), had a significantly smaller change in $\Delta\Psi_m$ (Fig. 5), and generated significantly less ROS (Fig. 6). In contrast, CH2 and L828 fibroblasts are very sensitive to CSE-induced apoptosis, highlighting the different susceptibilities of fibroblast strains from different human beings.

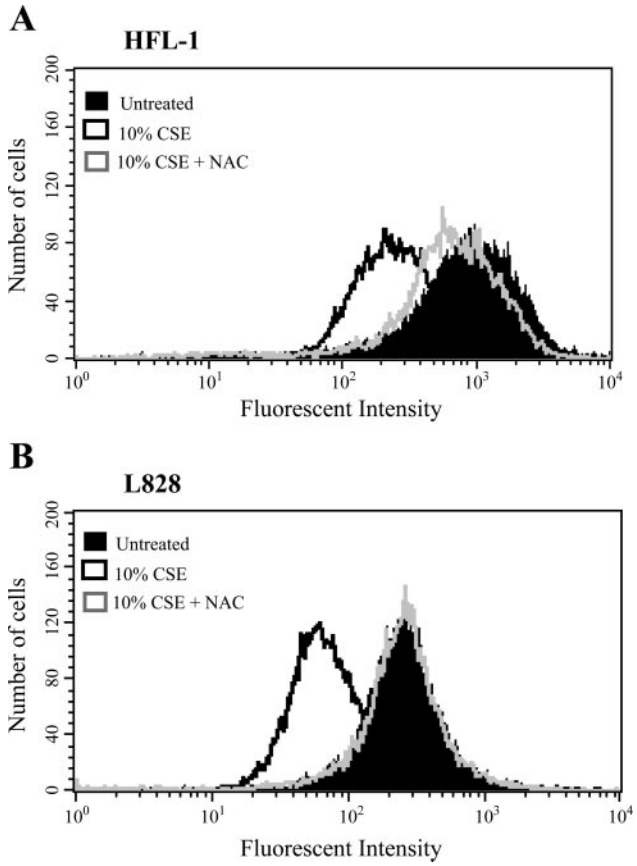

Fig. 9. CSE-induced loss of $\Delta\Psi_m$ is attenuated by treatment with 1 mM *N*-acetyl-L-cysteine (NAC). Human lung fibroblasts were untreated or cultured in the presence of 10% CSE for 6 h, and changes in mitochondrial $\Delta\Psi_m$ were assessed by flow cytometry as described in MATERIALS AND METHODS. At the highest concentration of CSE used, 10%, pretreatment with 1 mM NAC dramatically attenuated the loss of $DiOC_6$ incorporation as assessed by flow cytometry in human lung fibroblast strains HFL-1 (*A*) and L828 (*B*).

Fibroblasts are the main cell type in the lung interstitium, are involved in tissue repair and remodeling (63), provide structural support to the alveolar compartment, and are believed to be an important target of cigarette smoke-induced damage (4, 7, 19, 22, 26, 38). We previously showed (38) that low doses of CSE (i.e., nonapoptotic) elicit inflammatory mediators such as Cox-2, mPGES-1, and the prostaglandin PGE_2 from human lung fibroblasts, thereby contributing to the inflammatory milieu observed in the lungs of smokers. Chronic inflammation, resulting in the destruction of alveolar walls and development of emphysema (39, 55), may involve the depletion of alveolar structural cells through oxidative stress. Oxidative stress is increased in smokers and patients with COPD (35, 45, 48), initiates the early events in inflammation in the lung (35), and can directly trigger apoptosis (56, 58). Cigarette smoke contains an estimated 10^{17} oxidant molecules per puff (8), including aldehydes, quinones, nitric oxide, hydroxyl radical, and hydrogen peroxide and other free radicals (8, 35, 50). We have used H_2DCFDA, a nonfluorescent compound that is incorporated into the cell and oxidized to a fluorescent dye in the presence of ROS (11), to demonstrate that CSE induces ROS production in human lung fibroblasts, with the CH2 fibroblast strain exhibiting the highest levels of ROS after CSE exposure (Fig. 6). This increase in the oxidant burden to the lung may contribute significantly to the induction of apoptosis and loss of structural cells characteristic of emphysema. Furthermore, fibroblasts that have increased levels of ROS can release factors that induce apoptosis in overlying epithelial cells, which may result in further airway damage (56, 59).

A consequence of ROS production and the increased oxidative stress response associated with cigarette smoke is lipid peroxidation in the lungs. A specific end product of lipid peroxidation is 4-HNE, which can react with DNA and proteins to generate various adducts that can induce cellular responses, including apoptosis (52). 4-HNE has been shown to induce oxidative stress and apoptosis in 3T3 fibroblasts (31). Furthermore, 4-HNE adducts are increased in the lungs of subjects with COPD compared with those without (52). Thus we speculated that the oxidative stress we observed in CSE-treated fibroblasts would increase 4-HNE levels. Using immunocytochemistry, we have demonstrated for the first time that treatment with CSE increased 4-HNE levels in human lung fibroblasts (Fig. 7). Using an antibody against 4-HNE, we observed intense staining in the cytoplasm, nuclear membrane, and nucleus of smoke-treated fibroblasts, consistent with the ability of 4-HNE to diffuse within the cells and form adducts with cysteine, lysine, and histidine residues (27, 52). Thus membrane lipid peroxidation associated with increased ROS production may be contributing to the cigarette smoke-induced lung fibroblast apoptosis.

GSH is the principal antioxidant in the lung (23, 47), and we measured intracellular GSH levels in response to CSE. We show that GSH levels initially decrease in response to 5% CSE but are able to recover to control levels in some but not all fibroblast strains (Fig. 8). This indicates that lung fibroblasts from different individuals have intrinsically diverse capabilities to recover from acute exposure to an environmental pollutant such as cigarette smoke. Furthermore, the ability to recover GSH levels in the HFL-1 fibroblast strain correlates well with the resistance of this fibroblast strain to CSE-induced apoptosis. GSH depletion can induce apoptosis (17) through endogenously produced ROS (16). ROS can damage chromosomal DNA and other cellular components, leading to apoptosis (15). The ability of the HFL-1 fibroblast strain to recover GSH levels to near baseline correlates well with our observations that this fibroblast strain produced less ROS (Fig. 6) and was the least sensitive in terms of viability (Fig. 1). In contrast, the most sensitive fibroblast strain, CH2, exhibited a dramatic decline in viability at lower percentages of CSE and generated significantly more ROS compared with the other fibroblast strains, despite the fact that this strain did not exhibit significant changes in mitochondrial $\Delta\Psi_m$ (Fig. 5). CH2 fibroblasts were also unable to recover GSH levels (Fig. 8). Thus the enhanced sensitivity of this human lung fibroblast strain, but not the HFL-1 strain, to CSE may be the result of ROS-induced cellular damage caused by GSH depletion and not alterations in mitochondrial $\Delta\Psi_m$.

An increase in oxidative stress can lead to the oxidation of GSH to GSSG. CSE initiated an oxidative stress response in human lung fibroblasts, as determined by ROS production (Fig. 6) and lipid peroxidation (Fig. 7). Despite the decrease in GSH levels after CSE exposure to human lung fibroblasts, there was no concurrent increase in GSSG. Our results are in agreement with a previous study that demonstrated that both in vivo and in vitro exposure to cigarette smoke condensate deplete intra-

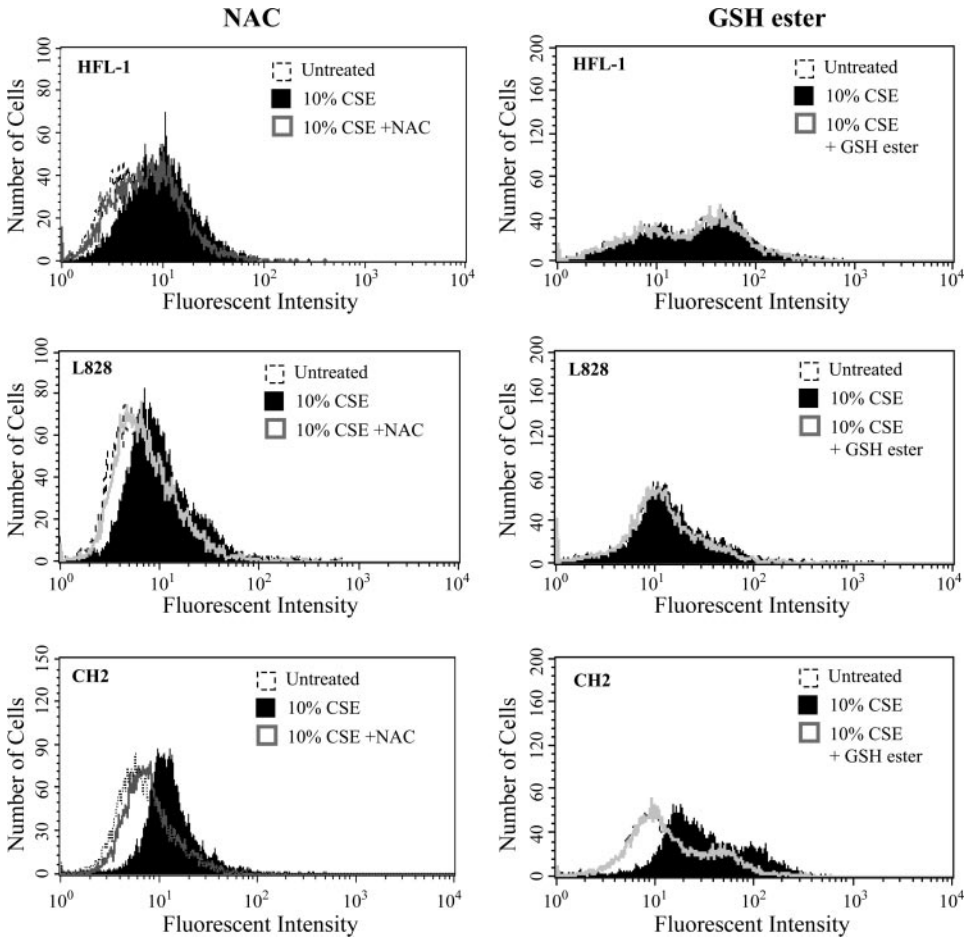

Fig. 10. CSE-induced generation of ROS is completely prevented by NAC and GSH ester. Fibroblast strains HFL-1, L828, and CH2 were preincubated with 1 mM NAC (*left*) or 5 mM GSH ester (*right*) followed by treatment with 10% CSE and analyzed by flow cytometry as described in MATERIALS AND METHODS. Fibroblasts that were exposed to 10% CSE exhibited an increase in ROS compared with control cells. The addition of both NAC and GSH ester prevented this increase in ROS to levels that were similar to fibroblasts that were untreated. Note the variability of CSE-induced ROS generation among the fibroblast strains.

cellular GSH without an elevation in GSSG, suggesting that the GSH depletion by cigarette smoke was not the result of direct oxidation (46). Rahman and colleagues (46) also demonstrated in the A549 alveolar epithelial cell line that there was an elevation in the level of GSH-conjugate formation and inhibition of activity of glutamate-cysteine ligase (GCL, formerly referred to as γ-glutamylcysteine synthetase), a key enzyme involved in GSH synthesis. Thus the depletion of GSH in CSE-treated human lung fibroblasts may be due to alterations in GSH biosynthesis.

The protective effects of exogenous GSH have been observed in vitro for H_2O_2-induced apoptosis and necrosis (56) and CSE-induced apoptosis in HFL-1 human lung fibroblasts (4). Furthermore, long-term administration of NAC to patients with COPD reduced H_2O_2 formation in the airways (25) and lowered the exacerbation rate in patients with chronic bronchitis (3). Here we report that CSE-induced ROS production and induction of apoptosis were dramatically attenuated with both GSH and the GSH precursor NAC (Figs. 9 and 10) in three different human lung fibroblast strains. Augmenting the levels of intracellular GSH may be therapeutically appropriate to treat patients with COPD by reducing the severity of oxidant-induced inflammation and alveolar wall cell apoptosis.

Oxidative stress and ROS are important inducers of the apoptotic pathway that involves changes in $\Delta\Psi_m$ (2, 18, 24). Mitochondria and thus $\Delta\Psi_m$ are required for cell survival, and an alteration in $\Delta\Psi_m$ is an early, irreversible, and universal event in the cell death process (10, 29, 62). Mitochondrial depolarization in response to cigarette smoke has been demonstrated for human mononuclear cells (2). We measured $\Delta\Psi_m$ with $DiOC_6$, a fluorescent dye that strongly labels mitochondria; a decrease in $\Delta\Psi_m$ is associated with reduced $DiOC_6$ uptake (42) and is thus indicative of apoptosis. In all fibroblast strains, cigarette smoke induced a reduction in $\Delta\Psi_m$ (Fig. 5). We also measured mitochondrial activity/viability with MTT. In all cases, there was a dramatic reduction in response to CSE (Figs. 1 and 2). At lower concentrations (i.e., concentrations that did not reduce viability), however, there was an increase in mitochondrial activity in fibroblast strains L828 (Fig. 1*B*) and HFL-1 (Fig. 1*A*), indicating mitochondrial hyperpolarization. In the CH2 fibroblast strain, viability steadily decreased at these lower concentrations (Fig. 1*C*), indicating greater sensitivity in this fibroblast strain. A transient increase in $\Delta\Psi_m$ after the induction of apoptosis has been observed in HeLa cells (33), retinal pigment epithelial cells (28), and Jurkat T cells (24, 60). Although the mechanism leading to this hyperpolarization is unknown, it appears to be an early event in the apoptotic cascade (33).

Apoptosis is also characterized by changes in the physical characteristics of a cell, which include nuclear condensation, membrane blebbing, and cell shrinkage. Conversely, necrosis is the result of cell injury and typically leads to an increase in cell volume because the membrane does not remain intact. Apoptosis can be distinguished from necrosis on the basis of

light scatter profiles measured by flow cytometry (62). We observed dramatic changes in fibroblast morphology after exposure to 10% CSE, including changes in cell size (Fig. 4). All fibroblast strains exhibited a clear decrease in forward scatter profiles, whereas the side scatter profile remained unchanged, indicative of a reduction in cell volume typical of the early stages of apoptosis (9, 62). Reduction in cell size based on forward scatter flow cytometric profile has also been observed in apoptotic human gingival fibroblasts treated with concanavalin A (30).

It has been proposed that genetic variability may account for the reason that only a proportion (~20%) of smokers develop COPD. Fibroblasts are an important target of cigarette smoke-induced lung disease, and their differential sensitivity to CSE-induced apoptosis may contribute to the development of COPD in some but not all patients. The results presented here clearly indicate that although all three fibroblast strains underwent CSE-induced apoptosis, there was significant variability in their sensitivity to CSE, as judged by viability, ROS production, and $\Delta\Psi_m$. Different fibroblast strains may have intrinsically diverse endogenous antioxidant capabilities and hence may be better able to deal with the increased oxidant burden to the lung that occurs as a result of cigarette smoking. Therapies aimed at increasing antioxidant levels by augmenting GSH levels may prove useful in combating CSE-related diseases such as emphysema.

GRANTS

This research was supported by National Institutes of Health Grants DE-011390, ES-01247, K08-HL-04492, and HL-075432; P. Morris USA, P. Morris International, and P. Morris Fellowship Program; and American Lung Association Grant DA004-N and Research Training Fellowship.

REFERENCES

1. **Aoshiba K, Tamaoki J, and Nagai A.** Acute cigarette smoke exposure induces apoptosis of alveolar macrophages. *Am J Physiol Lung Cell Mol Physiol* 281: L1392–L1401, 2001.
2. **Banzet N, Francois D, and Polla BS.** Tobacco smoke induces mitochondrial depolarization along with cell death: effects of antioxidants. *Redox Rep* 4: 229–236, 1999.
3. **Boman G, Backer U, Larsson S, Melander B, and Wahlander L.** Oral acetylcysteine reduces exacerbation rate in chronic bronchitis: report of a trial organized by the Swedish Society for Pulmonary Diseases. *Eur J Respir Dis* 64: 405–415, 1983.
4. **Carnevali S, Petruzzelli S, Longoni B, Vanacore R, Barale R, Cipollini M, Scatena F, Paggiaro P, Celi A, and Giuntini C.** Cigarette smoke extract induces oxidative stress and apoptosis in human lung fibroblasts. *Am J Physiol Lung Cell Mol Physiol* 284: L955–L963, 2003.
5. **Carp H and Janoff A.** Possible mechanisms of emphysema in smokers. In vitro suppression of serum elastase-inhibitory capacity by fresh cigarette smoke and its prevention by antioxidants. *Am Rev Respir Dis* 118: 617–621, 1978.
6. **Chakrabarti S, Vitseva O, Iyu D, Varghese S, and Freedman JE.** The effect of dipyridamole on vascular cell-derived reactive oxygen species. *J Pharmacol Exp Ther* 315: 494–500, 2005.
7. **Chen LJ, Zhao Y, Gao S, Chou IN, Toselli P, Stone P, and Li W.** Downregulation of lysyl oxidase and upregulation of cellular thiols in rat fetal lung fibroblasts treated with cigarette smoke condensate. *Toxicol Sci* 83: 372–379, 2005.
8. **Church DF and Pryor WA.** Free-radical chemistry of cigarette smoke and its toxicological implications. *Environ Health Perspect* 64: 111–126, 1985.
9. **Darzynkiewicz Z, Bruno S, Del Bino G, Gorczyca W, Hotz MA, Lassota P, and Traganos F.** Features of apoptotic cells measured by flow cytometry. *Cytometry* 13: 795–808, 1992.
10. **Debatin KM, Poncet D, and Kroemer G.** Chemotherapy: targeting the mitochondrial cell death pathway. *Oncogene* 21: 8786–8803, 2002.
11. **Deng M, Zhao JY, Ju XD, Tu PF, Jiang Y, and Li ZB.** Protective effect of tubuloside B on TNFα-induced apoptosis in neuronal cells. *Acta Pharmacol Sin* 25: 1276–1284, 2004.
12. **Fries KM, Sempowski GD, Gaspari AA, Blieden T, Looney RJ, and Phipps RP.** CD40 expression by human fibroblasts. *Clin Immunol Immunopathol* 77: 42–51, 1995.
13. **Griffith OW.** Determination of glutathione and glutathione disulfide using glutathione reductase and 2-vinylpyridine. *Anal Biochem* 106: 207–212, 1980.
14. **Grzelak A, Rychlik B, and Bartosz G.** Light-dependent generation of reactive oxygen species in cell culture media. *Free Radic Biol Med* 30: 1418–1425, 2001.
15. **Higuchi Y.** Chromosomal DNA fragmentation in apoptosis and necrosis induced by oxidative stress. *Biochem Pharmacol* 66: 1527–1535, 2003.
16. **Higuchi Y.** Glutathione depletion-induced chromosomal DNA fragmentation associated with apoptosis and necrosis. *J Cell Mol Med* 8: 455–464, 2004.
17. **Higuchi Y and Matsukawa S.** Glutathione depletion induces giant DNA and high-molecular-weight DNA fragmentation associated with apoptosis through lipid peroxidation and protein kinase C activation in C6 glioma cells. *Arch Biochem Biophys* 363: 33–42, 1999.
18. **Hoidal JR.** Reactive oxygen species and cell signaling. *Am J Respir Cell Mol Biol* 25: 661–663, 2001.
19. **Holz O, Zuhlke I, Jaksztat E, Muller KC, Welker L, Nakashima M, Diemel KD, Branscheid D, Magnussen H, and Jorres RA.** Lung fibroblasts from patients with emphysema show a reduced proliferation rate in culture. *Eur Respir J* 24: 575–579, 2004.
20. **Horwath-Winter J, Simon M, Kolli H, Trummer G, and Schmut O.** Cytotoxicity evaluation of soft contact lens care solutions on human conjunctival fibroblasts. *Ophthalmologica* 218: 385–389, 2004.
21. **Hoshino Y, Mio T, Nagai S, Miki H, Ito I, and Izumi T.** Cytotoxic effects of cigarette smoke extract on an alveolar type II cell-derived cell line. *Am J Physiol Lung Cell Mol Physiol* 281: L509–L516, 2001.
22. **Ishii T, Matsuse T, Igarashi H, Masuda M, Teramoto S, and Ouchi Y.** Tobacco smoke reduces viability in human lung fibroblasts: protective effect of glutathione *S*-transferase P1. *Am J Physiol Lung Cell Mol Physiol* 280: L1189–L1195, 2001.
23. **Jardine H, MacNee W, Donaldson K, and Rahman I.** Molecular mechanism of transforming growth factor (TGF)-β_1-induced glutathione depletion in alveolar epithelial cells. Involvement of AP-1/ARE and Fra-1. *J Biol Chem* 277: 21158–21166, 2002.
24. **Kadenbach B, Arnold S, Lee I, and Huttemann M.** The possible role of cytochrome *c* oxidase in stress-induced apoptosis and degenerative diseases. *Biochim Biophys Acta* 1655: 400–408, 2004.
25. **Kasielski M and Nowak D.** Long-term administration of *N*-acetylcysteine decreases hydrogen peroxide exhalation in subjects with chronic obstructive pulmonary disease. *Respir Med* 95: 448–456, 2001.
26. **Kim H, Liu X, Kobayashi T, Conner H, Kohyama T, Wen FQ, Fang Q, Abe S, Bitterman P, and Rennard SI.** Reversible cigarette smoke extract-induced DNA damage in human lung fibroblasts. *Am J Respir Cell Mol Biol* 31: 483–490, 2004.
27. **Kim HJ, Liu X, Wang H, Kohyama T, Kobayashi T, Wen FQ, Romberger DJ, Abe S, MacNee W, Rahman I, and Rennard SI.** Glutathione prevents inhibition of fibroblast-mediated collagen gel contraction by cigarette smoke. *Am J Physiol Lung Cell Mol Physiol* 283: L409–L417, 2002.
28. **Kim JM, Bae HR, Park BS, Lee JM, Ahn HB, Rho JH, Yoo KW, Park WC, Rho SH, Yoon HS, and Yoo YH.** Early mitochondrial hyperpolarization and intracellular alkalinization in lactacystin-induced apoptosis of retinal pigment epithelial cells. *J Pharmacol Exp Ther* 305: 474–481, 2003.
29. **Kroemer G.** Mitochondrial control of apoptosis: an introduction. *Biochem Biophys Res Commun* 304: 433–435, 2003.
30. **Kulkarni GV, Lee W, Seth A, and McCulloch CA.** Role of mitochondrial membrane potential in concanavalin A-induced apoptosis in human fibroblasts. *Exp Cell Res* 245: 170–178, 1998.
31. **Kutuk O, Adli M, Poli G, and Basaga H.** Resveratrol protects against 4-HNE induced oxidative stress and apoptosis in Swiss 3T3 fibroblasts. *Biofactors* 20: 1–10, 2004.
32. **Li L, Hamilton RF Jr, Taylor DE, and Holian A.** Acrolein-induced cell death in human alveolar macrophages. *Toxicol Appl Pharmacol* 145: 331–339, 1997.
33. **Li PF, Dietz R, and von Harsdorf R.** p53 regulates mitochondrial membrane potential through reactive oxygen species and induces cyto-

chrome *c*-independent apoptosis blocked by Bcl-2. *EMBO J* 18: 6027–6036, 1999.
34. **Loo DT and Rillema JR.** Measurement of cell death. *Methods Cell Biol* 57: 251–264, 1998.
35. **Macnee W and Rahman I.** Oxidants and antioxidants as therapeutic targets in chronic obstructive pulmonary disease. *Am J Respir Crit Care Med* 160: S58–S65, 1999.
36. **Maeno E, Ishizaki Y, Kanaseki T, Hazama A, and Okada Y.** Normotonic cell shrinkage because of disordered volume regulation is an early prerequisite to apoptosis. *Proc Natl Acad Sci USA* 97: 9487–9492, 2000.
37. **Martey CA, Baglole CJ, Gasiewicz TA, Sime PJ, and Phipps RP.** The aryl hydrocarbon receptor is a regulator of cigarette smoke induction of the cyclooxygenase and prostaglandin pathways in human lung fibroblasts. *Am J Physiol Lung Cell Mol Physiol* 289: L391–L399, 2005.
38. **Martey CA, Pollock SJ, Turner CK, O'Reilly KM, Baglole CJ, Phipps RP, and Sime PJ.** Cigarette smoke induces cyclooxygenase-2 and microsomal prostaglandin E_2 synthase in human lung fibroblasts: implications for lung inflammation and cancer. *Am J Physiol Lung Cell Mol Physiol* 287: L981–L991, 2004.
39. **Marwick JA, Kirkham P, Gilmour PS, Donaldson K, MacNee W, and Rahman I.** Cigarette smoke-induced oxidative stress and TGF-β_1 increase $p21^{waf1/cip1}$ expression in alveolar epithelial cells. *Ann NY Acad Sci* 973: 278–283, 2002.
40. **Numanami H, Koyama S, Nelson DK, Hoyt JC, Freels JL, Habib MP, Amano J, Haniuda M, Sato E, and Robbins RA.** Serine protease inhibitors modulate smoke-induced chemokine release from human lung fibroblasts. *Am J Respir Cell Mol Biol* 29: 613–619, 2003.
41. **Odaka C and Ucker DS.** Apoptotic morphology reflects mitotic-like aspects of physiological cell death and is independent of genome digestion. *Microsc Res Tech* 34: 267–271, 1996.
42. **Ozgen U, Savasan S, Buck S, and Ravindranath Y.** Comparison of $DiOC_6(3)$ uptake and annexin V labeling for quantification of apoptosis in leukemia cells and non-malignant T lymphocytes from children. *Cytometry* 42: 74–78, 2000.
43. **Pauwels RA, Buist AS, Calverley PM, Jenkins CR, and Hurd SS.** Global strategy for the diagnosis, management, and prevention of chronic obstructive pulmonary disease. NHLBI/WHO Global Initiative for Chronic Obstructive Lung Disease (GOLD) Workshop summary. *Am J Respir Crit Care Med* 163: 1256–1276, 2001.
44. **Platoshyn O, Zhang S, McDaniel SS, and Yuan JX.** Cytochrome *c* activates K^+ channels before inducing apoptosis. *Am J Physiol Cell Physiol* 283: C1298–C1305, 2002.
45. **Rahman I.** The role of oxidative stress in the pathogenesis of COPD: implications for therapy. *Treat Respir Med* 4: 175–200, 2005.
46. **Rahman I, Li XY, Donaldson K, Harrison DJ, and MacNee W.** Glutathione homeostasis in alveolar epithelial cells in vitro and lung in vivo under oxidative stress. *Am J Physiol Lung Cell Mol Physiol* 269: L285–L292, 1995.
47. **Rahman I and MacNee W.** Lung glutathione and oxidative stress: implications in cigarette smoke-induced airway disease. *Am J Physiol Lung Cell Mol Physiol* 277: L1067–L1088, 1999.
48. **Rahman I and MacNee W.** Oxidant/antioxidant imbalance in smokers and chronic obstructive pulmonary disease. *Thorax* 51: 348–350, 1996.
49. **Rahman I and MacNee W.** Oxidative stress and regulation of glutathione in lung inflammation. *Eur Respir J* 16: 534–554, 2000.
50. **Rahman I and MacNee W.** Role of oxidants/antioxidants in smoking-induced lung diseases. *Free Radic Biol Med* 21: 669–681, 1996.
51. **Rahman I, Mulier B, Gilmour PS, Watchorn T, Donaldson K, Jeffery PK, and MacNee W.** Oxidant-mediated lung epithelial cell tolerance: the role of intracellular glutathione and nuclear factor-κB. *Biochem Pharmacol* 62: 787–794, 2001.
52. **Rahman I, van Schadewijk AA, Crowther AJ, Hiemstra PS, Stolk J, MacNee W, and De Boer WI.** 4-Hydroxy-2-nonenal, a specific lipid peroxidation product, is elevated in lungs of patients with chronic obstructive pulmonary disease. *Am J Respir Crit Care Med* 166: 490–495, 2002.
53. **Repine JE, Bast A, and Lankhorst I.** Oxidative stress in chronic obstructive pulmonary disease. Oxidative Stress Study Group. *Am J Respir Crit Care Med* 156: 341–357, 1997.
54. **Sauer H, Klimm B, Hescheler J, and Wartenberg M.** Activation of p90RSK and growth stimulation of multicellular tumor spheroids are dependent on reactive oxygen species generated after purinergic receptor stimulation by ATP. *FASEB J* 15: 2539–2541, 2001.
55. **Snider GL.** Chronic obstructive pulmonary disease: risk factors, pathophysiology and pathogenesis. *Annu Rev Med* 40: 411–429, 1989.
56. **Teramoto S, Tomita T, Matsui H, Ohga E, Matsuse T, and Ouchi Y.** Hydrogen peroxide-induced apoptosis and necrosis in human lung fibroblasts: protective roles of glutathione. *Jpn J Pharmacol* 79: 33–40, 1999.
57. **Tietze F.** Enzymic method for quantitative determination of nanogram amounts of total and oxidized glutathione: applications to mammalian blood and other tissues. *Anal Biochem* 27: 502–522, 1969.
58. **Tuder RM, Petrache I, Elias JA, Voelkel NF, and Henson PM.** Apoptosis and emphysema: the missing link. *Am J Respir Cell Mol Biol* 28: 551–554, 2003.
59. **Uhal BD, Joshi I, True AL, Mundle S, Raza A, Pardo A, and Selman M.** Fibroblasts isolated after fibrotic lung injury induce apoptosis of alveolar epithelial cells in vitro. *Am J Physiol Lung Cell Mol Physiol* 269: L819–L828, 1995.
60. **Vander Heiden MG, Chandel NS, Williamson EK, Schumacker PT, and Thompson CB.** Bcl-xL regulates the membrane potential and volume homeostasis of mitochondria. *Cell* 91: 627–637, 1997.
61. **Vayssier M, Banzet N, Francois D, Bellmann K, and Polla BS.** Tobacco smoke induces both apoptosis and necrosis in mammalian cells: differential effects of HSP70. *Am J Physiol Lung Cell Mol Physiol* 275: L771–L779, 1998.
62. **Vermes I, Haanen C, and Reutelingsperger C.** Flow cytometry of apoptotic cell death. *J Immunol Methods* 243: 167–190, 2000.
63. **Wong LS, Green HM, Feugate JE, Yadav M, Nothnagel EA, and Martins-Green M.** Effects of "second-hand" smoke on structure and function of fibroblasts, cells that are critical for tissue repair and remodeling. *BMC Cell Biol* 5: 13, 2004.
64. **Yang YM and Liu GT.** Damaging effect of cigarette smoke extract on primary cultured human umbilical vein endothelial cells and its mechanism. *Biomed Environ Sci* 17: 121–134, 2004.